JOURNAL OF THE PHYSIOAL SOCIETY OF JAPAN Vol. 17, SUPPLEMENT A-II, 1962
INTERNATIONAL CONFERENCE ON COSMIC RAYS AND THE EARTH STORM Part II

II-2-6. Correlation between Outer Radiation Belt and Solar-Geophysical Phenomena

Sekiko YOSHIDA,

Physical Institute, Nagoya University, Nagoya, Japan

Nobuo MATUURA,

Radio Research Laboratories, Kokubunji, Tokyo, Japan

AND

Takesi NAGATA

Geophysical Institute, Tokyo University, Tokyo, Japan

The study of time variations of the outer radiation belt may be highly important in relation to its origin. This paper has been prepared for the understanding of their mechanism. Since the discovery of the radiation belts by Van Allen, it has been well known that flux intensity of the outer radiation belt varies appreciably in association with magnetic storms.

To study the mechanism of such flux variation, the data as listed in the Table was used. In this Table, the onset times of the solar flare events and their subsequent magnetic storms are listed, and occurrence of phenomena such as polar cap blackout and solar cosmic rays associated with each solar flare are shown. Further, sums of K_p indices for one day intervals before and after the onset of each solar flare are shown, and it should be noticed that such ΣK_p may represent magnetic activity before the beginning of magnetic storm corresponding to the solar flare. Concerning the data in the Table, it may be regarded that the occurrence of unusual in-

Table of Solar and Terrestrial Disturbances

No.	Data Reference of Flux Intensity	Position of Obs. Alt. km	Solar Flare Onset Time (U. T.)	Geomagnetic Storm ssc (U. T.)	P.C.B.	S.C.R.	ΣKp	S.R.B. Index
1	Rothwell *et al.*[1] Exp. IV	2000—2200	1958, Aug. 16, 04:32	Aug. 17, 06:23	yes	yes	20_o	5
2	〃	1281—1985	1958, Sep. 2, 10:40	Sep. 3, 08:43	no	no	9_+	1
3	Van Allen *et al.*[2] Pion. III	equator	1958, Dec. 3, 05:58	Dec. 4, 00:35	no	no data	20_o	1
4*	Van Allen *et al.*[3] Pion. IV	equator	1959, Feb. 27, 22:26	Feb. 24, 23:19 Mar. 2, 08:24(si?)	no ($f_{\min}$ increase)	no data	40_-	2
5	Arnoldy *et al.*[4] Exp. VI Fan *et al.*[5] Exp. VI	equator	1959, Aug. 14, 00:44	Aug. 16, 04:04	no	yes (small)	12_+	1
6*	〃	〃	Aug. 17, 20:48	Aug. 20, 04:12	yes	yes	42_-	2
7	〃	〃	Sep. 3, 04:21	Sep. 3, 14:17 or 3, 21:59	no	yes (small)	28_-	3
8	Van Allen *et al.*[6] Exp. VII Arnoldy *et al.*[7] Pion. V Fan *et al.*[8] Pion. V	~1000	1960, Mar. 30, 14:55	Mar. 31, 08:15	yes	no	27_o	5
9*	〃	〃	Apr. 1, 08:45	Apr. 2, 23:03	yes	yes	66_+	5
10*	〃	〃	Apr. 5, 02:15	Apr. 6, 16:35	yes	yes	34_o	5
11	〃	〃	Apr. 9, 01:23	Apr. 10, 01:27	no	no	25_o	2

P. C. B.: Polar cap blackout   S. C. R.: Solar cosmic rays in the exosphere

S. R. B. Ind.: Solar radio burst index (after T. Takakura[9])

* unusual increase of flux intensity in the outer radiation belt was observed

crease of flux intensity in the outer radiation belt is possible only when two necessary conditions are satisfied simultaneously, namely, only when onset of solar flare, such as those accompanied by polar cap blackout and solar cosmic rays, chances to coincide with magnetically active periods on the earth. In practice, such conditions may be satisfied when the solar flares occur successively having a shorter interval than, perhaps, several days. Therefore, we may get an idea of the mechanism of increase in the outer radiation belt, namely, high energy particles are ejected from the sun on the occasion of intense solar flare, and that such particles arriving at the earth some time later, can penetrate deep into the earth's exosphere under the influence of a widely extended irregular magnetic field, which may naturally exist during magnetically active period.

Time sequences of peak intensity variation in the outer radiation belt as well as solar and geophysical phenomena are shown in Fig. 1. Among five cases, two of them show a clear increase after solar flare which occurred during a magnetic storm, and on the other hand, the remaining three cases when effective solar flare did not occur, show no unusual increase but do show recovery in parallel manner with horizontal component of *Dst* field. In all five cases, the decrease of peak intensity in a similar manner with *Dst* field can be seen, except for the increase effect mentioned above. In Fig. 2, peak intensity variations presenting unusual increases are plotted with smoothed curves and they clearly show the increase of peak intensity during the interval between solar flare and subsequent magnetic storm.

Time variation on radial distribution of intensity obtained by R. L. Arnoldy *et al.*[4] is shown in Fig. 3. Radial distributions of ratio of pulse number from ion chamber to count number from G-M counter are shown in the bottom figure correspondingly to four stages (a)—(d), where stage (d) corresponds to on August 24. In stage (b), the effect of decrease is stronger for lower energy particles than for higher energy particles in the region beyond 15,000 km from earth's center. In stage (c), the increase effect is stronger

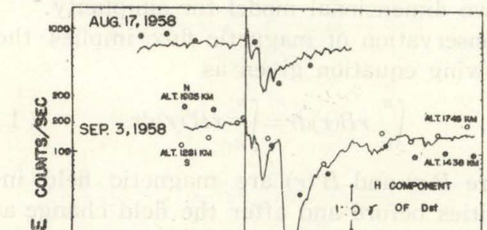

Fig. 1. Peak intensity of the outer radiation belt is plotted for five storm periods. Continuous lines represent horizontal component of *Dst* field reduced from hourly values.

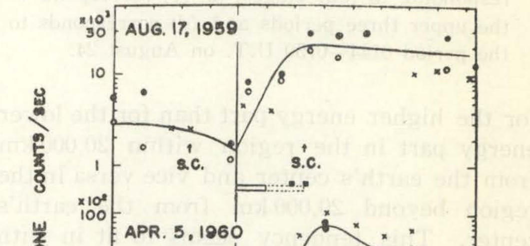

Fig. 2. Peak intensity of the outer radiation belt for three cases arranging the onset time of each solar flare.

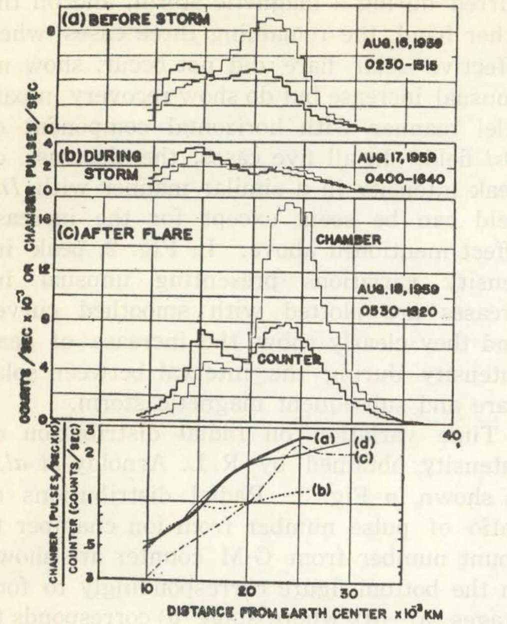

Fig. 3. Upper three figures show radial distribution of flux intensity observed by G-M counter and ion chamber (after R. L. Arnoldy *et al.*[4]). Bottom figure shows the radial distribution of ratio of pulse number to count number corresponding to four stages, (a)-(c) correspond to the upper three periods and (d) corresponds to the period 0144—0750 U.T. on August 24.

for the higher energy part than for the lower energy part in the region within 20,000 km from the earth's center and vice versa in the region beyond 20,000 km from the earth's center. This tendency seems to fit in with the idea of particle penetration. In stage (d), the energy spectrum becomes almost equal to that of stage (a) though flux intensities for both energy parts are still much above normal levels. On the other hand, the results obtained from scintillation counter measurements of which energy is approximately >200 Kev, show an unusual increase of flux intensity instead of decrease after the beginning of the magnetic storm on August 16 as was recently reported by A. Rosen and T. A. Farley.[10] These lower energy particles may be a part of the solar corpuscular stream causing the magnetic storm which corresponds to the solar flare on August 14.

Decrease of flux intensity for particles in Mev range associated with magnetic storm is always observed, and intensity variation is similar to the horizontal component of *Dst* field unless effect of unusual increase acts upon it. Such close relation between variations of flux intensity and of *Dst* field suggests some kinds of direct influences of *Dst* field upon flux intensity. They are, (1) change in geometry of geomagnetic field lines, or expansion of tubes of field lines during main phase, (2) change in energy of each particle owing to field change, (3) change in pitch angle of each particle, (4) change in B/B_0, where B_0 is field intensity of a certain field line at the equator and B is field intensity at a point on the same field line. Among these four effects based on the assumption of adiavatic change, effects of (3) and (4) contribute to a little raise of mirror point, and it is not so important for the decreasing effect of flux intensity, and the effect of (2) is comparable to or less than that of (1), although it depends on the sharpness of energy dependence for instrumental cut-off and of the energy spectrum of trapped particles. Therefore, the effect of expansion near the equatorial plane will be discussed in two dimensional model for simplicity.

Conservation of magnetic flux implies the following equation given as

$$\int_{R_0}^{R} rB(r)dr=\int_{R_0'}^{R'} rB'(r)dr\ , \qquad (1)$$

where $B(r)$ and $B'(r)$ are magnetic field intensities before and after the field change at radial distance r and the limits of integration are fixed on the same line of force in both state before and after field change. Similarly, conservation of the number of particles which are frozen into the field lines implies the following equation given as

$$\int_{R_0}^{R} rN(r)dr=\int_{R_0'}^{R'} rN'(r)dr\ . \qquad (2)$$

Further, on the same field line, we can obtain the following relation as

$$N(R)/N'(R')=B(R)/B'(R')\ . \qquad (3)$$

In practice, we may put R_0 in Eqs. (1) and (2) equal to zero and then R_0' becomes equal to zero. Calculation has been done in two cases; (I) Using Eqs. (1) and (3), when $B(r)$, $B'(r)$ and $N(r)$ are given by the centered dipole field, the centered dipole field superposed by the radially uniform *Dst* field and the radial distribution of number density (is proportional to flux intensity) given in Fig. 3(a), respectively. (II) Using Eqs. (2) and (3), when $B(r)$, $N(r)$ and $N'(r)$ are given by the centered dipole field, the radial distribution of number densities shown in Fig. 3, (a) and (b), respectively. Results obtained in case (I) are compared with the observational results in Fig. 4. In Fig. 5, the top figure shows the comparison between observed (on August 16–17) and calculated (case (I)) flux distribution with radial distance, and this shows a good agreement between them when depressed *Dst* field of 300 gammas is taken; however, the observed *Dst* field on the ground at the same period was about 130 gammas. Such a discrepancy as seen in lower figure of Fig. 4 and in top figure in Fig. 5 may be convinced from the observational result reported by E. J. Smith[11]

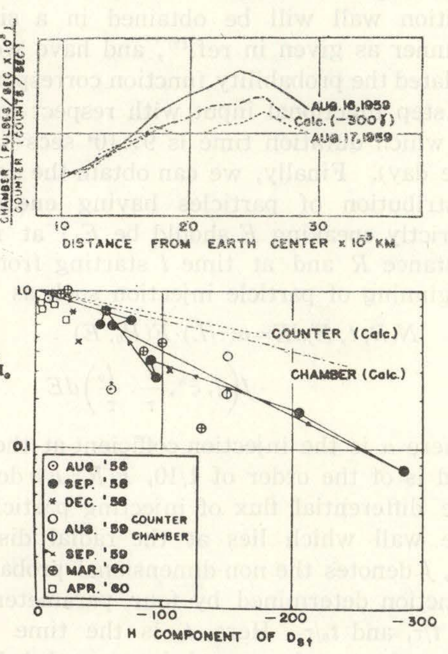

Fig. 4. Upper figure shows the ratio of pulse number to count number corresponding to before storm (continuous line), during storm (decreased flux intensity; dotted line) and calculated flux intensity assuming −90 and −300 gammas *Dst*. Lower figure shows the relation between flux intensity ratio I/I_0 (I_0: normal intensity; I: storm time intensity) and horizontal component of *Dst* field reduced from hourly values corresponding to the same time when I is observed. Dotted and broken lines are obtained from calculation.

that *Dst* field of about 350 gammas at 4 earth radii has been observed on August 17, with Explorer VI. The middle and bottom figures of Fig. 5 show the calculated *Dst* field (case (II)) in linear and logarithmic scale, respectively. The obtained result near the inner edge of density profile may have a considerable amount of error caused by numerical integration from ambiguous density distribution near the inner edge of the profile.

The problem of diffusive penetration of charged particles into the exosphere under the influence of an irregular magnetic field as observed with space vehicles by C. P. Sonett *et al.*[12] has been discussed by N. Matuura and T. Nagata[13] to explain the origin

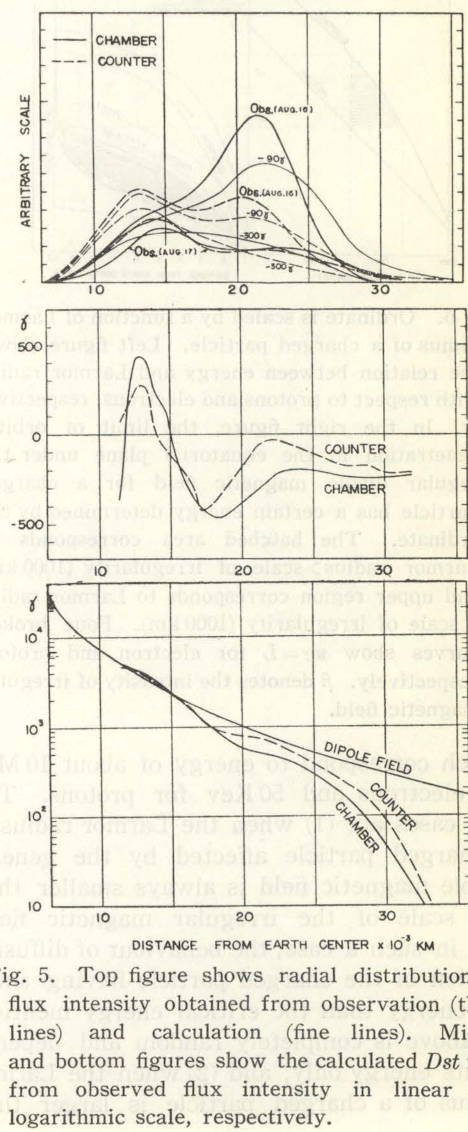

Fig. 5. Top figure shows radial distribution of flux intensity obtained from observation (thick lines) and calculation (fine lines). Middle and bottom figures show the calculated *Dst* field from observed flux intensity in linear and logarithmic scale, respectively.

of the ring current corresponding to the main phase of a magnetic storm. Application of this idea to the origin of trapped particles in the outer radiation belt will be examined. Characteristics of the irregular magnetic field excited during a magnetic storm throughout the exosphere are simply assumed such that linear scale, $L=1000$ km, life time $\tau=10$ secs, and field intensity of the effective irregular magnetic field $\beta=1-10$ gammas. Behaviour of charged particle motion under the influence of an irregular magnetic field can be separated into two cases, and in the middle figure of Fig. 6, the separation is shown critically by lateral broken lines

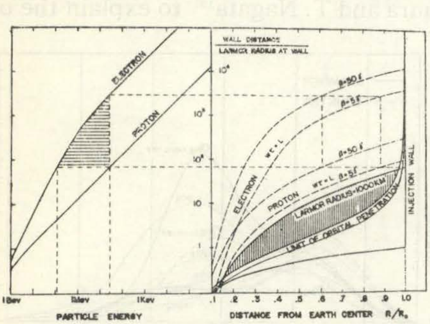

Fig. 6. Ordinate is scaled by a function of Larmor radius of a charged particle. Left figure shows the relation between energy and Larmor radius with respect to protons and electrons, respectively. In the right figure, the limit of orbital penetration in the equatorial plane under the regular dipole magnetic field for a charged particle has a certain energy determined by the ordinate. The hatched area corresponds to Larmor radius > scale of irregularity (1000 km) and upper region corresponds to Larmor radius < scale of irregularity (1000 km). Four broken curves show $w\tau=L$ for electron and proton, respectively. β denotes the intensity of irregular magnetic field.

which correspond to energy of about 10 Mev for electrons and 50 Kev for protons. The two cases are (1) when the Larmor radius of a charged particle affected by the general dipole magnetic field is always smaller than the scale of the irregular magnetic field, and in such a case, the behaviour of diffusive motion of the charged particle having smaller energy than the critical energy mentioned above is completely random and depends on its energy only, and (2) when the Larmor radius of a charged particle is larger than the scale of the irregular magnetic field, and in such a case, the behaviour of diffusive motion of the charged particle having higher energy than the critical energy appears in small angle scattering and depends on its Larmor radius. From simple estimation, the effect of penetration and trapping is most predominant for particles corresponding to particles near the critical energy and the electron abundance in the outer radiation belt may easily be persuaded from Fig. 6. In case (1), which seems realistic for particles consisting of the outer radiation belt, velocity of random motion may be given by random drift velocity w owing to gradient of irregular magnetic field, as treated in ref.[13], but with respect to the length of one step, here we will put $w\tau$ and L corresponding to the cases as $w\tau<L$ and $w\tau>L$, respectively. The probability function corresponding to the impulsive input at the injection wall will be obtained in a similar manner as given in ref.[13], and have we calculated the probability function corresponding to step functional input with respect to time of which duration time is 9×10^4 secs (about one day). Finally, we can obtain the density distribution of particles having energy E (strictly speaking E should be $E_\perp$) at radial distance R and at time t starting from the beginning of particle injection such as

$$N(R,t,E)dE=\alpha(\tau/L)\cdot F(R_0,E)\cdot J\left(\xi,\xi^*,\frac{t}{\tau},\frac{t_0}{\tau}\right)dE\,, \qquad (4)$$

where α is the injection cofficient at the wall and is of the order of 1/10, $F(R_0,E)$ denotes the differential flux of injecting particles at the wall which lies at the radial distance R_0, J denotes the non-dimensional probability function determined by four parameters, ξ, ξ^*, t/τ, and t_0/τ. Here, t_0 is the time duration of step functional input and ξ,ξ^* are given by

$$\xi = R/R_0$$

and

$$\xi^*=\left(\frac{a}{R_0}\right)\cdot\left(\frac{eB_0{}^2L^2}{E\tau\beta}\right)^{1/6}. \qquad (5)$$

The symbols a, e, β and B_0 are earth's radius, electric charge of particles, intensity of irregular magnetic field and intensity of earth's general magnetic field at the surface of the earth. The thus obtained probability function J, putting $a/R_0=1/10$, can be compared with observed results such as time variation of peak intensity in Fig. 7 and position of peak intensity in Fig. 8. As seen in Fig. 7,

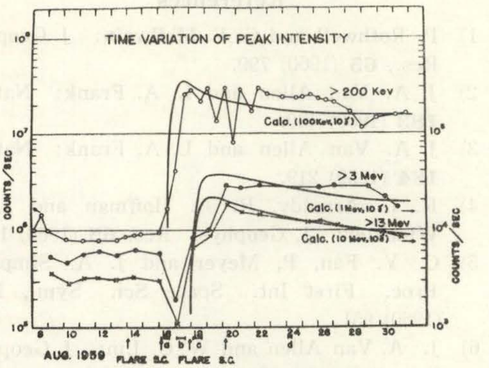

Fig. 7. Comparison of time variation of peak intensity between observation and calculation obtained from step functional solar particle injection of which duration is assumed to be 9×10^4 secs.

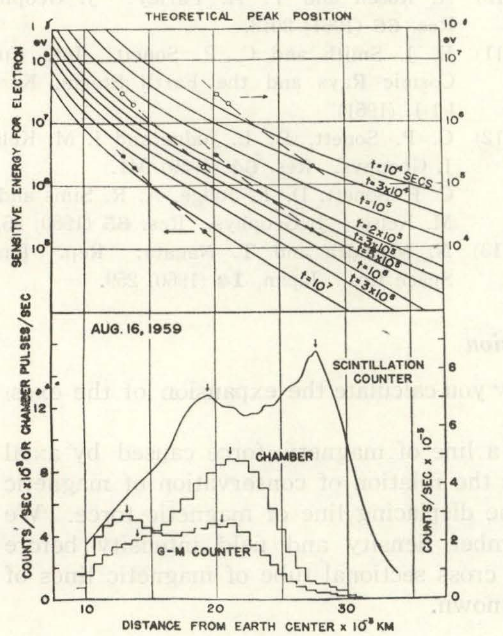

Fig. 8. Upper figure shows the feature of time variation of peak position for the particles having various energies and broken curves show the energy dependence of peak position obtained from lower figure. Lower figure shows radial flux distribution obtained from observation on three kinds of measurement (after R. L. Arnoldy *et al.*[4]) C. Y. Fan *et al.*[5]) and A. Rosen *et al.*[10])).

the beginning of injection for particles measured with scintillation counter (>200 Kev) should be regarded at the onset of SSC on August 16. In Fig. 8, the radial distribution peak position with respect to particle energy is compared between observed and calculated results. Though the origin of two separated peaks is still uncertain, fairly good agreement may be seen under the influence of 1—10 gammas irregular magnetic field. An example of the probability function J is shown in Fig. 9 where E=1 Mev, β=5 gammas, and the peak value of J on the order

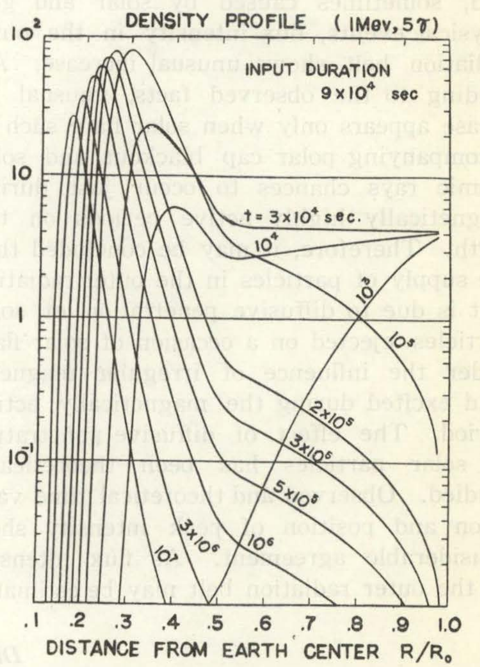

Fig. 9. Curves show the time variation of probability function after injection of solar particles for the case of E=1 Mev and β=5 gammas.

of 10^2 is attained a day after the injection. Then the peak flux intensity corresponding to this energy can be given approximately from Eq. (4) by

$$F_{\text{peak}} \approx 10^4 F(R_0)\,. \qquad (5)$$

Therefore, concerning the observed low flux intensity in interplanetary space as reported by R. L. Arnoldy *et al.*[7] we may not come to a conclusion that the source of the outer radiation belt should be sought in the exosphere.

Conclusion

Storm time variation of flux intensity in the outer radiation belt may be separately considered as two mechanisms. At first, the flux intensity of trapped particles above Mev range has a variation directly connected with *Dst* field there during magnetic storms, except for the gradual decrease of flux intensity caused by leakage of trapped particles owing to atmospheric scattering. Such decrease phenomena may be well explained by the exospheric expansion effect which is directly connected with *Dst* field and there is considerable agreement in quantity between observed and calculated results. Second, sometimes caused by solar and geophysical events, flux intensity in the outer radiation belt shows unusual increase. According to the observed facts, unusual increase appears only when solar flare such as accompanying polar cap blackout and solar cosmic rays chances to occur just during magnetically highly active periods on the earth. Therefore, it may be concluded that the supply of particles in the outer radiation belt is due to diffusive penetration of solar particles ejected on a occasion of solar flare under the influence of irregular magnetic field excited during the magnetically active period. The effect of diffusive penetration of solar particles has been theoretically studied. Observed and theoretical time variation and position of peak intensity show considerable agreement. As flux intensity in the outer radiation belt may be estimated as order of four times higher than the flux intensity of solar particles, the low flux in interplanetary space observed by Pioneer V may not contradict our idea of solar origin.

References

1) P. Rothwell and C. E. McIlwain: J. Geophys. Res., **65** (1960) 799.
2) J. A. Van Allen and L. A. Frank: Nature, **183** (1959) 430.
3) J. A. Van Allen and L. A. Frank: Nature, **184** (1959) 219.
4) R. L. Arnoldy, R. A. Hoffman and J. R. Winckler: J. Geophys. Res. **65** (1960) 1361.
5) C. Y. Fan, P. Meyer and J. A. Simpson: Proc. First Int. Space Sci. Sym., Nice, (1960) 951.
6) J. A. Van Allen and W. C. Lin: J. Geophys. Res. **65** (1960) 2998.
7) R. L. Arnoldy, R. A. Hoffman and J. R. Winckler: J. Geophys. Res. **65** (1960) 3004.
8) C. Y. Fan, P. Meyer and J. A. Simpson: J. Geophys. Res. **65** (1960) 1862.
9) T. Takakura: private communication
10) A. Rosen and T. A. Farley: J. Geophys. Res. **66** (1961) 2013.
11) E. J. Smith and C. P. Sonett: Int. Conf. Cosmic Rays and the Earth Storm, Kyoto, I-1-1, (1961)
12) C. P. Sonett, D. L. Judge and J. M. Kelso: J. Geophys. Res. **64** (1959) 941.
C. P. Sonett, D. L. Judge, A. R. Sims and J. M. Kelso: J. Geophys. Res. **65** (1960) 55.
13) N. Matuura and T. Nagata: Rep. Ionos. Space Res. Japan, **14** (1960) 259.

Discussion

Singer, S. F.: Could you elaborate on how you calculate the expansion of the exosphere?

Matuura, N.: The radial displacement of a line of magnetic force caused by axial symmetric *Dst* field can be obtained from the relation of conservation of magnetic flux integrated from the earth's center to the displacing line of magnetic force. We can also obtain one of the two ratios of number density and field intensity before and after displacement at a certain small cross sectional tube of magnetic lines of force by the use of another ratio which is known.